



1 **CO₂ partial pressure and CO₂ emissions from the lower** 2 **Red River (Vietnam)**

3 Thi Phuong Quynh Le^{1*}, Cyril Marchand^{2,3}, Cuong Tu Ho⁴, Thi Thuy Duong⁴, Huong
4 Thi Mai Nguyen¹, Lu XiXi⁵, Duy An Vu¹, Phuong Kieu Doan¹ and Nhu Da Le¹

5 ¹: Institute of Natural Product Chemistry, Vietnam Academy of Science and Technology, 18 Hoang
6 Quoc Viet Road, Cau Giay, Hanoi, Vietnam.

7 ²: IMPMC, Institut de Recherche pour le Développement (IRD), UPMC, CNRS, MNHN, Noumea,
8 New Caledonia, France.

9 ³: Faculty of Chemistry, University of Science – VNUHCM, 225 Nguyen Van Cu, Ho Chi Minh City,
10 Vietnam

11 ⁴: Institute of Environmental Technology, Vietnam Academy of Science and Technology, 18 Hoang
12 Quoc Viet Road, Cau Giay, Hanoi, Vietnam.

13 ⁵: Department of Geography, National University of Singapore, Arts Link 1, Singapore 117570,
14 Singapore.

15
16 *Correspondence to:* Thi Phuong Quynh Le (quynhltp@yahoo.com or quynhltp@gmail.com)

17 **Abstract.** The Red River (Vietnam) is a good example of a South-East Asian river system, strongly
18 affected by climate and human activities. This study aims to quantify the spatial and seasonal
19 variability of carbon dynamic and CO₂ outgassing at the water-air interface of the lower Red River
20 system. The monitoring of water quality and CO₂ emission were carried out for 24h cyclings at the five
21 stations during the dry and monsoon seasons. The riverine water *p*CO₂ was supersaturated with CO₂ in
22 contrast to the atmospheric equilibrium (400 ppm), averaging about 1588.6 ± 884.6 ppm, thus resulting
23 in a water–air CO₂ flux of 26.9 ± 18.4 mmol m⁻² day⁻¹. The CO₂ outgassing rate was characterized by
24 significant spatial variations, highest at Hoa Binh station (Da River) due to the dam impoundment and
25 the highest river flow. Surprisingly, CO₂ outgassing was higher in the day time (30.4 ± 21.2 mmol m⁻²
26 day⁻¹) than in the night time (23.3 ± 15.4 mmol m⁻² day⁻¹), probably as a result of the combined effect
27 of higher wind speed and water temperature in the day time. Seasonal differences were also observed,
28 higher in the wet season (30.7 ± 23.1 mmol m⁻² day⁻¹) than in the dry season (23.0 ± 12.2 mmol m⁻²
29 day⁻¹), due to higher river discharges and higher external inputs of organic matters from watersheds.
30 Conversely during dry season, temperature was among the main factors influencing C dynamic, with
31 higher *p*CO₂ and fluxes, probably as a result of increased metabolic rates.

32 **Keywords:** carbon, CO₂ outgassing, Red River, Vietnam

33

34 **1 Introduction**

35 Natural hydrological processes and biogeochemistry of many rivers in the world have suffered from the
36 influences of climate change and human activities in their drainage basins. Riverine carbon fluxes and
37 outgassing are important parts of the carbon exchange among terrestrial, oceanic and atmospheric
38 environment. Rivers and streams not only transfer various forms of carbon (dissolved and particulate)
39 to oceans, but also evade a significant amount of carbon to the atmosphere (Battin et al., 2009; Richey



40 et al., 2002). Due to CO₂ evasion, the flux of carbon that leaves the terrestrial biosphere through global
41 fluvial network was suggested to be twice larger than the amount that ultimately reaches the coastal
42 ocean (Bauer et al., 2013; Regnier et al., 2013). The existence of hotspot of CO₂ evasion represented 70
43 % of the emission for only 20 % of the land surface (Raymond et al., 2013). Previous estimates
44 proposed that inland water bodies transport, mineralize and bury 2.7 Pg C yr⁻¹, which is similar to the
45 terrestrial carbon sink for anthropogenic emissions of 2.8 Pg C yr⁻¹ (Tranvik et al., 2009). However,
46 more recent studies proposed a lower value of global evasion rate from inland waters, being about 2.1
47 Pg C yr⁻¹ or even less (Raymond et al., 2013; Lauerward et al., 2015).

48 Carbon fluxes and emissions from rivers are impacted by both natural (plate margin tectonics,
49 volcanic deposits, high elevations, steep slopes, and high intensive rainfall) and anthropogenic factors
50 (high population density, deforestation, reservoir impoundment, intensive agricultures, and
51 urbanization). However, there is a limited understanding of spatial and temporal dynamics of carbon
52 exchange between terrestrial, oceanic and atmospheric environments for the large Asian rivers. In
53 southeast Asia, the river water discharge and sediment loads have been altered dramatically over the
54 past decades as a result of reservoir impoundment, land use, population, and climate changes (Walling
55 and Fang, 2003, 2006; Lu, 2004). Solid sediment loads not only directly contribute to increase the
56 organic carbon content, but also affect chemical weathering and hence carbon consumption and
57 possible carbon emission. Therefore, studies of carbon emission from the large Asian rivers are crucial
58 to quantify geochemical cycles accurately in the context of global change. Some studies noted that data
59 concerning CO₂ evasion (or *p*CO₂) of Southeast Asian rivers is a high priority in order to precise the
60 global evasion rate from inland water (Raymond et al., 2013; Lauerward et al., 2015).

61 The Red River with a basin area of 156,450 km² is a typical East Asia river that is strongly
62 affected by climate and human activities (Fig. 1). Previous studies reported about the hydrology and
63 suspended sediment load associated to some elements loads (N, P, C) of the Red River (Dang et al.,
64 2010; Lu et al., 2015; Le et al., 2015). Recently, the transfer of organic carbon of the Red River to
65 ocean has been studied (Dang et al., 2010; Le et al., 2017). However, the knowledge of carbon
66 exchange at the air-water interface of the Red River is still limited.

67 This study aims: i) to investigate spatial and temporal (wet and dry, and day-night) variations of CO₂
68 partial pressure (*p*CO₂) and CO₂ flux at the water-air surface of the lower Red River, from the
69 upstream to the downstream part; and ii) to identify some of the factors that may control *p*CO₂ and
70 CO₂ outgassing rates of the lower Red River. To our knowledge, the present study introduced the first
71 measurement and estimation of CO₂ evasion from the lower Red River.

72 2 Methods

73 2.1 Study sites

74

75 Five stations were studied in the lower Red River (Vietnam): Yen Bai, Hoa Binh, Vu Quang, Hanoi
76 and Ba Lat (Fig. 1). Yen Bai station was located at the outlet of the Thao river; Hoa Binh station (after
77 Son La and Hoa Binh reservoirs) at the outlet of the Da River; Vu Quang at the outlet of the Lo River;



78 Hanoi and Ba Lat in the main course of the Red River downstream. The Ba Lat station is located in the
79 Red River mouth, about 50 km from the sea.

80 The climate in the Red River basin, of tropical East Asia monsoon type, is controlled by the
81 North East monsoon in winter and South West monsoon in summer. It is, thus, characterized by two
82 distinct seasons: rainy and dry season. The rainy season lasts from May to October and cumulates 85 –
83 90 % of the total annual rainfall in the Red River catchment, whereas the dry season covers the period
84 from November to next April. The monsoon climate weather results in a hydrologic regime
85 characterized by large runoffs during the wet season and low runoffs during the dry season (see below
86 for the detail river discharge in 2014). A series of dams-reservoirs are impounded in both Chinese and
87 Vietnamese territories of the Red River upstream part (Le et al., 2017). In the Da River, two large
88 dams Hoa Binh and Son La were constructed in the river main course whereas in the Lo River, two
89 large dams Thac Ba and Tuyen Quang were constructed in its tributaries.

90 The upstream part of the Red River in the Chinese part is dominated by mountain areas, which
91 are tectonically active and unstable, and this, combined with intense rainfall, causes high erosion
92 (Fullen et al., 1998) whereas in the Vietnamese part, soils are mostly (70 %) grey and alluvial soils (Le
93 et al., 2017).

94 Land use was quite different in the three upstream river basins Thao, Da and Lo: Industrial
95 crops dominate (58 %) in the Lo basin, forests and bare land (74 %) in the Da basin, and paddy rice
96 fields (66 %) in the delta area. The Thao basin is characterized by a larger diversity of land use
97 including forest, paddy rice fields, and industrial crops (85 %) (Le et al., 2015).

98 Population density varied from the upstream to the downstream part of the Red River basin.
99 The delta area, where the Hanoi and Ba Lat stations are located, is characterized by high population
100 density (> 1,000 inhabitant km²). In the upstream part, where the Yen Bai station (in Thao River), Hoa
101 Binh station (in Da River) and Vu Quang station (in Lo River) situate, population density was much
102 lower, about 100 inhabitants km⁻² (Le et al., 2015).

103 2.2 Sampling procedures and analysis

104 Sampling campaigns were conducted in September (rainy season) and November (dry season) 2014 at
105 the five gauging stations.

106 Physico-chemical parameters were automatically recorded at the interval of 1 min during 24h
107 for each sampling campaign: pH, turbidity, salinity, chlorophyll *a* by the sensor YSI6920 (YSI, USA);
108 temperature and dissolved oxygen (DO) by a HOBO sensor (USA). These sensors have been calibrated
109 with standard solutions before each measurement campaign. All solutions used for calibration should
110 be at ambient temperature to ensure quality of calibration and all data must be entered on the
111 documents.

112 In parallel of in-situ measurement, river water samples were hourly collected for analysis of
113 other water quality variables (TSS, DOC, POC, and alkalinity) during 24h. A known volume of well-
114 mixed sample was filtered immediately by vacuum filtration through pre-combusted (at 450 °C for 6 h)
115 glass fiber filters (Whatman GF/F, 47 mm diameter). The filters were then kept in a freezer (-20 °C)
116 until analysis of TSS and POC. For the measurement of TSS, each filter was dried for 1h at 105 °C and



117 then weighed. Taking into account the filtered volume, the increase in weight of the filter represented
118 the total TSS per unit volume (mg L^{-1}).

119 POC concentrations were estimated on the same filters. Filters were then weighed before and
120 after calcination at $550\text{ }^{\circ}\text{C}$ for 4 hours. The difference in weight before and after calcination was
121 multiplied by 0.4 to provide an estimation of the POC content (Servais et al., 1995).

122 A volume of 30 ml sub-sample of filtrate was acidified with $35\text{ }\mu\text{l}$ $85\text{ }\%$ H_3PO_4 acid and then
123 stored at $4\text{ }^{\circ}\text{C}$ in amber glass bottles until measurement of the DOC concentrations using a TOC- V_E
124 (Shimadzu, Japan). The samples, standards and blank measurements were measured in triplicate.

125 Total alkalinity was hourly determined on non-filtered water samples in situ by titration method
126 (APHA, 1995).

127 Wind speed and air temperature were measured hourly during 24 h of all sampling campaigns
128 by a hand digital thermometer/anemometer (GM 8901, Total meter, Taiwan).

129 **2.3 Hydrological data collection**

130 Daily and hourly data of river water discharges in 2014 at the 5 hydrological stations studied were
131 collected from the Vietnam Ministry of Natural Resources and Environment (MONRE, 2016). The
132 daily data were collected for all days in 2014, whereas hourly data were obtained for the exact dates of
133 field measurements at the 5 sites (Table 1). The mean annual river flows in 2014 of the Thao, Da, Lo
134 Rivers and in the main axe of the Red River at the Hanoi and Ba Lat stations were: 527 ± 515 ; $1369 \pm$
135 833 ; 1302 ± 517 ; 1867 ± 1089 ; $615 \pm 293\text{ m}^3\text{ s}^{-1}$, respectively. Higher values of river discharges were
136 observed in wet season (May to October) than in dry season (January-April; November-December) at
137 all sites (Table 1).

138 **2.4 CO₂ fluxes determination**

139 CO₂ fluxes were determined using direct methods: i) from $p\text{CO}_2$ in the water column measured using
140 an equilibrator connected to an IRGA ii) from $p\text{CO}_2$ determined by the calculation using T_{alk} and pH
141 measured in-situ.

142

143 **2.4.1 From measured $p\text{CO}_2$**

144 Equilibrator was used to determine the $p\text{CO}_2$ in water balanced with the air. The equilibrator was
145 designed, as described in Frankignoulle et al. (2001), as follow: a vertical plastic tube (height: 73 cm,
146 diameter: 9 cm) which is filled up with about 250 glass marbles (diameter = 1.5 cm) in order to
147 increase the surface exchange between water and air. The river water (water inlet) through a submerged
148 pump at 20 cm below the river surface water comes into the equilibrator from the top of the tube. The
149 water inlet can be regulated by a flow controller installed under the tygon tubing, which joins the water
150 inlet with the pump. A closed air circuit ensures circulation through the equilibrator (from the bottom
151 to the top), a water trap, a particle filter, a regulator and an IRGA (Licor 820, Licor[®], USA), which was
152 calibrated before each sampling campaign using a series of standards concentrations of 0, 551 and 2756
153 ppm CO₂ (Air Liquide[®]). The IRGA was connected to a computer interface, which allows recording
154 the $p\text{CO}_2$ every second. Values were recorded during 24 h continuously.



155 The water-air CO₂ fluxes from the equilibrator measurement at each site were calculated by
156 the formula proposed by Raymond and Cole (2011) as followings:

$$157 F_{\text{Equi}} = k_{600} * \alpha * (p\text{CO}_2 \text{ water} - p\text{CO}_2 \text{ air}) \quad \text{Eq. (1)}$$

158 Where F was the CO₂ flux from water ($\mu\text{mol m}^{-2} \text{ s}^{-1}$) and converted in $\text{mmol m}^{-2} \text{ d}^{-1}$;

159 k_{600} , was gas transfer velocity of CO₂ or piston velocity (cm h^{-1}), and was calculated according to a
160 wind speed function (k vs. U_{10}). k_{600} was calculated using the equation from Raymond and Cole
161 (2001), which developed from a data set of different estuaries and rivers as follow:

$$162 k_{600} = 1.91 \times \exp(0.35 \times U_{10}) \times (Sc / 600)^{-0.5} \quad \text{Eq. (2)}$$

163 Where U_{10} was the wind speed (m s^{-1}) at 10 m height above the surface water (was calculate
164 from the wind speed (m s^{-1}) at 2 m height, ("Appendix 8.6-Wind Speed Calculations" 2010); and Sc
165 was the Schmidt number, normalized to Schmidt number of 600 (Cole and Caraco, 1998).

166 α was the solubility coefficient of CO₂ for given temperature and salinity (Weiss, 1974) (mol
167 $\text{L}^{-1} \text{ atm}^{-1}$). In this case, $\alpha = 0.034 \text{ mol L}^{-1} \text{ atm}^{-1}$

168 $p\text{CO}_2 \text{ water}$ was CO₂ concentration in surface river water from Equilibrator measurement or
169 from CO₂_SYS calculation.

170 $p\text{CO}_2 \text{ air}$ was considered as a constant of 400 ppm

171 Since we measured wind speed on field at a height of 2 meters ($U_z = 2$) with a handle
172 anemometer, the formula of Amorochio and DeVries (1980) was used to estimate the wind speed at 10
173 m height (U_{10}).

174 The determination of the emissions depends on the gas exchange velocities (k_{600}), and the
175 latter may represent a considerable source of uncertainty when calculating water-air CO₂ outgassing
176 flux (Raymond et al., 2012; Raymond et al., 2013). There were some studies focused on the estimation
177 of k_{600} , based on empirical equations with different techniques (Jähne et al., 1984; Liss and Merlivat,
178 1986), for different type of ecosystems and specific weather conditions (Devol et al., 1987; Marino and
179 Howarth, 1993; Clark et al., 1995; Carini et al., 1996; Guérin et al., 2007; Vachon et al., 2010). As a
180 result, different empirical equations have been proposed, which lead to different quantitative
181 estimations of k_{600} coefficient. In our study, we decided to use the empirical equation of k_{600} -wind from
182 Raymond and Cole (2001) developed from a data set of different estuaries and rivers.

183 Some studies indicate that k_{600} values are closely related to flow velocity and channel gradient
184 for rivers (Alin et al., 2011), less related to wind velocity as in lakes and oceans (Abril et al., 2000;
185 Abril and Borges, 2004; Abril et al., 2009) and that water current can strongly affect the magnitude of
186 k_{600} , especially in location where the wind speed is low but water current is high (Borges et al., 2003).
187 In our study, k_{600} is determined by the Eq. (2) on which a wind speed function (k vs. U_{10}) strongly
188 affected that may lead to underestimate k_{600} . The underestimation of k_{600} may lead to lower CO₂ flux
189 out-gassing. Thus, we consider that the CO₂ outgassing fluxes in our study reflected likely a low
190 estimate.



191

192 **2.4 From calculated $p\text{CO}_2$**

193 DIC content may be calculated from the sum of total dissolved inorganic carbon in water including
194 HCO_3^- , CO_3^{2-} , H_2CO_3 and CO_2 , or can be calculated from a combination of any two of the following
195 measured parameters total alkalinity, pH, or partial pressure of CO_2 ($p\text{CO}_2$) (Cai et al., 2008; Sun et al.,
196 2010). In this study, DIC contents were calculated from the sum of including HCO_3^- , CO_3^{2-} , H_2CO_3
197 and CO_2 contents, which were given by the calculation from the CO_2 -SYS Software (version 2.0)
198 basing on the total alkalinity contents and pH values measured in-situ as described above (Sect. 2.3).

199 In order to compare with $p\text{CO}_2$ in water, which was measured by the equilibrator, $p\text{CO}_2$ in
200 water at the 5 sites was also simultaneously calculated on the CO_2 -SYS EXCEL Macro Software
201 basing on total alkalinity contents and pH values measured in-situ at the 5 sites as described above
202 (Sect. 2.3).

203 We feel confident about our measurements of $p\text{CO}_2$, because both methods yielded similar
204 results.

205 **2.5. Statistical analysis**

206 To detect the correlation between environmental variables and $p\text{CO}_2$ or CO_2 outgassing flux, statistical
207 software R version 3.3.2 (R Core Team, 2016) was applied to calculate the Pearson correlation
208 coefficients. Some environmental variables were evaluated by “cor” to compare the correlation and
209 selected representative variables. PCA analysis was then used for identifying representative variables
210 that could relate to the dynamic of $p\text{CO}_2$ or CO_2 flux.

211

212 **3. Results**213 **3.1. Physical and chemical variables of the lower Red River**

214 Water temperature varied from 23.3 to 29.4 °C, and the mean value in rainy period (27.4 °C) was
215 higher than the one in dry period (24.5 °C) at almost all stations, except at the Hoa Binh site where the
216 water temperatures did not show seasonal variations, remaining around 26.3 - 26.5 °C. Among the five
217 hydrological stations, the higher water temperatures were recorded at the Hanoi and Ba Lat stations,
218 ranging from 28 to 29 °C in the wet period, whereas they were close to 23 °C during the dry period.
219 Temperatures at the Yen Bai and Vu Quang stations were approximately 26 °C in the wet period and 24
220 °C in the dry period (Table 2, Fig. 2).

221 pH values were not hugely different among the two periods. pH was slightly basic, ranging
222 from 7.7 to 8.2 with an average 8.1 for all the sites. The lowest pH values were observed at the Hoa
223 Binh in both periods (< 8), whereas they ranged between 8.0 and 8.4 at the other sites. pH was slightly
224 higher in dry season than in the wet season at all the sites (Table 2, Fig. 2). The percentage of dissolved
225 oxygen (% DO) varied from 50.5 to 70.7 % with an average value of 64.3 %. There were not
226 significant differences in % DO with season, 63.6 % during the rainy seasons and 64.9 during the dry



227 season (Table 2). The mean values were the highest for the Yen Bai station (70.1 %) in the wet period,
228 and 69.5 % for the Ba Lat station in the dry period. The lowest values were observed at the Hoa Binh
229 station in both periods (55.0 % in the wet period, 51.4% in the dry period) (Table 2, Fig. 2).

230 Salinity at the four upstream sites was under the detection limit both in the rainy and dry
231 seasons, but in the estuary downstream river at the Ba Lat station, values up to 8.75 were measured
232 during the dry season (Table 2).

233 Alkalinity concentrations ranged from 84.3 ± 1.9 to 152.9 ± 6.6 mg L^{-1} , with higher values in the
234 dry season than in the rainy season, except at Vu Quang station. Conductivity ranged from 0.2 ± 0.0 to
235 6.6 ± 3.4 mS cm^{-1} , but did not show a clear variation between the dry and rainy season (Table 2, Fig. 2).

236 Chlorophyll *a* was quite low during the two sampling campaigns, ranging from 0.23 to 2.77
237 $\mu\text{g L}^{-1}$, with an average of $1.61 \mu\text{g L}^{-1}$. Higher values in the rainy season than in the dry season were
238 observed at almost sites. From Yen Bai to Ba Lat, Chl-*a* concentrations in the main axe (at Yen Bai and
239 Hanoi stations) were higher than in the two tributaries Da and Lo (Table 2, Fig. 2), even under the
240 higher values of turbidity.

241 The wind speed ranged from 0.2 ± 0.3 to 3.1 ± 1.5 m s^{-1} , and the highest value occurred in the
242 dry season at Ba Lat. The results showed a clear variation in wind speed between day and night, with
243 the higher values during the day time for all stations (Table 3).

244 3.2. Carbon concentrations of the lower Red River

245 During the two sampling campaigns, DOC concentration ranged from 0.5 to 4.6 mgC L^{-1} , averaging 1.5
246 mgC L^{-1} . Higher values were observed during the rainy season (2.0 mgC L^{-1} vs. 1.5 mgC L^{-1} during the
247 dry season), and the highest value was recorded at Hanoi site (Table 2). POC concentrations varied
248 from 0.4 to 4.6 mgC L^{-1} . The mean value in the rainy season was 1.6 mgC L^{-1} , slightly higher than in
249 dry season (1.4 mgC L^{-1}). Among the 5 sites, POC concentrations in the main reach of the Red River
250 (Yen Bai, Hanoi and Ba Lat sites) were higher than in the two tributaries Da and Lo, where dams were
251 constructed (Table 2, Fig. 2).

252 DIC concentrations at the five sites fluctuated from 16.7 to 32.9 mgC L^{-1} , averaging 23.8 mgC
253 L^{-1} . Lower values were observed in the rainy season (22.3 mgC L^{-1}), lower than the values in the dry
254 season (25.3 mgC L^{-1}) (Table 2, Fig. 2).

255

256 3.3. Comparisons of the $p\text{CO}_2$ results for the two methods

257 $p\text{CO}_2$ along the lower Red River (Vietnam) in the dry and monsoon seasons were determined by two
258 methods: i) direct measurements using an equilibrator connected to an IRGA, ii) calculated from pH
259 and alkalinity using the $\text{CO}_2\text{-SYS}^{\text{®}}$ software. The direct measurements gave higher values than the
260 calculated (Table 2), but the values of two methods were well correlated ($R^2 = 0.76$, Fig. 3). This result



261 is opposite to what was observed in organic-rich freshwater (Abril et al., 2015) or in estuarine
262 mangrove waters (Leopold et al., 2017), where large overestimation of the calculated $p\text{CO}_2$ was
263 observed. The higher calculated values compared to direct measurements were related to a more
264 significant contribution of organic acids anions to total alkalinity in waters with low carbonate
265 alkalinity and high DOC concentrations, and to a lower buffering capacity of the carbonate system at
266 low pH (Abril et al., 2015). However along the Red River, pH values remained around 8 and DOC
267 concentrations were lower than 2 mg L^{-1} (Table 2), which may explain for the lower calculated $p\text{CO}_2$
268 values (Table 2). Thus, in this study, we used the results of the measured $p\text{CO}_2$ for the discussion and
269 to determine the CO_2 emissions from the lower Red River to the atmosphere (Fig. 4).

270

271 3.4. Daily variations of $p\text{CO}_2$ and CO_2 emissions

272 The riverine water $p\text{CO}_2$ was supersaturated with CO_2 in contrast to the atmospheric equilibrium (400
273 ppm), averaging $1,588.6 \pm 884.6$ ppm. In general, the results did not show a clear variation in $p\text{CO}_2$
274 between the day and night at all stations, except higher values at the night time in the dry season at the
275 Ba Lat site (Table 2, Fig. 2).

276 CO_2 flux values in the day time were higher than in the night time for all the stations during
277 all sampling campaigns (Table 3, Fig. 4). Previous studies revealed that photosynthesis of
278 phytoplankton may have a strong influence on circadian variation of CO_2 outgassing, since this process
279 consumes CO_2 during the day (Linn and Doran, 1984; Cole et al., 2000). However, in the present study,
280 very low Chl-a concentrations were measured, from 0.5 to $3.1 \mu\text{g L}^{-1}$, probably as a result of the high
281 turbidity limiting light penetration in the water column. Thus, phytoplankton activity had a low
282 influence on C dynamic in the lower Red River system.

283 In the present study, water temperature was slightly higher in the day time than in the night
284 time (around $0.1 - 0.5 \text{ }^\circ\text{C}$) (Table 2), and positive correlations between temperature and CO_2 flux was
285 observed at Hoa Binh and Yen Bai station ($R^2 = 0.72$ and 0.84 , respectively). Water temperature could
286 alter the riverine $p\text{CO}_2$ value. Previous studies indicated that CO_2 water solubility decreases with the
287 temperature increase during the day (Parkin and Kaspar, 2003; Roulet et al., 1997), leading to higher
288 CO_2 outgassing from river water interface. This effect was observed for some rivers in the world
289 (Roulet et al., 1997; Guasch et al., 1998; Dornblaser and Striegl, 2013). However for the Ba Lat site,
290 CO_2 fluxes were higher during the day but it was not always the case for $p\text{CO}_2$, suggesting that another
291 factors may be responsible for these results. The other parameter that differed during the night and day
292 was the wind speed which was higher during the day (Table 3). Previous studies suggested that the
293 large changes of CO_2 fluxes observed between the day and night can be caused not only by biological
294 cycle but also mainly by daily wind patterns (Hamilton et al., 1994). Small changes in wind pattern
295 may modify the direction and magnitude of the CO_2 flux during the day-night cycle (Sellers et al.,
296 1995). Our results were in agreement with some reports for rivers in tropical region (e.g. the Shark
297 River in USA (Ho et al., 2016)), which emphasised the influence of strong diurnal signal in wind speed
298 leading to higher k values in the day time than in night time (Rey et al., 2012; Ho et al., 2016).



299 Different explanations were given for the day-night variation of $p\text{CO}_2$ and CO_2 flux for
300 aquatic ecosystems in the world. Ho et al. (2016) found higher CO_2 flux in the Shark River (USA)
301 during the day than at night was due to the strong diurnal signal in u_{10} . Similar results have also been
302 reported for the Yangtze River Delta (China) (Xu et al., 2017). Roulet et al. (1997) reported that CO_2
303 flux in some ponds in Canada were always higher during the day because of higher water
304 temperature. Higher CO_2 concentrations in day time were also observed for the two second-order
305 Mediterranean streams: Riera Major, a siliceous shaded stream and La Solana, a calcareous open
306 stream where changes in CO_2 concentration was greatly influenced by stream metabolism (Guasch et
307 al., 1998). However, average CO_2 outgassing during the night higher than during day by up to 1.8 times
308 was also observed for the Alpine streams, where temperature and hydrology were major drivers of
309 $p\text{CO}_2$ dynamics (Peter et al., 2014). CO_2 increased in the night time with the values of 6-46% higher
310 than the day time values during each 24-h period have been described by Sellers et al. (1995) for the
311 lake Northwest Ontario, Canada. Thus, it is possible that the contrast between day and night time
312 concentrations being a consequence of specific features of the measuring sites (Wang et al., 2010).

313 3.5. Seasonal variations of $p\text{CO}_2$ and CO_2 emission

314 $p\text{CO}_2$ values fluctuated from 694 ppm (at Yen Bai) in the dry season to 3,887 ppm (at Hoa Binh) in the
315 wet season. The mean values were highest for the Hoa Binh site in both seasons whereas the lowest one
316 was observed at the Yen Bai site. Higher values of $p\text{CO}_2$ in the wet season than in the dry season were
317 observed at almost sites, except at Yen Bai (Table 2).

318 CO_2 flux values varied with seasons, and ranged from $4.4 \pm 2.0 \text{ mmol m}^{-2} \text{ d}^{-1}$ (at Vu Quang) in the dry
319 season to $48.4 \pm 23.4 \text{ mmol m}^{-2} \text{ d}^{-1}$ (at Hoa Binh) in the wet season. CO_2 flux values were higher in the
320 wet season for all stations (Table 3, Fig. 4). During the monsoon season, the river discharges were
321 about 2 to 3 times higher at all the sites (Table 1). As known in tropical regions, the wet season usually
322 experienced higher $p\text{CO}_2$ than the dry season because of the intense rainfall that induces higher OM
323 inputs into the river. This process was observed in some subtropical rivers: the Longchuan River (Li et
324 al., 2012) and the Xijiang River (Yao et al., 2007), with $p\text{CO}_2$ values increasing significantly when
325 baseflow and interflow increased, and flushed significant amount of carbon into the streams. In
326 addition, it was suggested a link between the seasonal variation in soil CO_2 content and riverine CO_2
327 outgassing due to porewater export (Hope et al., 2004; Melack et al., 2009; Rudorff et al., 2011). Thus
328 the higher $p\text{CO}_2$ values observed along the lower Red River during the rainy season may reflect the
329 influence of soil organic matter inputs to the riverine water column, evidenced by the higher values of
330 DOC and POC in the rainy seasons at all the sites.

331

332 In addition, seasonal variation of temperature may also explain the seasonal variability of
333 $p\text{CO}_2$ values of the Red River, being higher during the hot rainy season. Some authors suggested that
334 higher water temperatures in wet season in tropical regions were responsible for increased $p\text{CO}_2$ and
335 higher CO_2 emissions towards the atmosphere (Chanda et al., 2013; Takahashi et al., 2002). Dessert et
336 al., (2003) suggested that higher temperature should induce higher weathering rates, leading to higher



337 DIC export. This effect was not only observed in tropical rivers but also in mixed mangrove forest in
338 India (Chanda et al., 2013), or in the Southern Ocean (Nomura et al., 2014). Increase in temperature
339 decreases CO₂ solubility but increase OM decomposition processes, which produce CO₂. This may
340 partly explain the higher *p*CO₂ of the Red River during the hot rainy season. However, direct
341 relationship between temperature and *p*CO₂ during the rainy season was not evident, probably because
342 riverine inputs were the dominant factor driving *p*CO₂, while during the dry season *p*CO₂ clearly
343 increased with temperature, suggesting that metabolic rate controlled *p*CO₂ when adjacent soils inputs
344 are limited (Fig. 5).

345 4. Discussion

346 PCA and Pearson correlation coefficient were performed to analyze the relationships between nine
347 environmental variables and *p*CO₂ or CO₂ evasion flux at five sampling stations of the lower Red River
348 in the wet season (September 2014) and dry season (November 2014). The PCA of the seasonal data
349 for five sampling stations presented a clear separation between two periods: rainy and dry season (Fig.
350 6). The rainy period was characterized by high levels of temperature, *p*CO₂, CO₂ flux, POC, DOC and
351 Chl *a*. The Pearson correlation coefficient showed a low positive correlation between *p*CO₂ and DIC
352 and oxygen saturation (%) ($r = 0.19$) and between CO₂ flux and DOC (0.17). Both *p*CO₂ and CO₂ flux
353 were found to be negatively correlated with pH ($r = -0.3$) (Table 4).

354 Consequently, we suggest that the *p*CO₂ and CO₂ outgassing are the results of a combination
355 of multiple parameters, rather than a single one: season (including precipitation and temperature), dam
356 construction, population density, geomorphological characteristics of the catchment, etc.

357

358 4.1. Influence of dams on *p*CO₂ and CO₂ emission

359 Along the lower Red River, *p*CO₂ values were characterized by significant spatial variations (Table 2,
360 Fig. 2). In the upstream part, *p*CO₂ ranged from 964 to 3,830 ppm. Within the three tributaries, in
361 addition to the two large dams (Hoa Binh and Son La) in the Vietnamese part, a series of dams in the
362 Chinese territory were constructed in the 2000s for the Da River, whereas only some small
363 dams/reservoirs were built up in the Thao River in the Chinese territory. In the present study, the
364 highest *p*CO₂ values and the lower pH values were measured at the Hoa Binh site, which is situated
365 downstream a series of reservoirs. Previously, reservoirs were suggested to decrease river *p*CO₂ due to
366 increased residence times and autotrophic production (Wang et al., 2007). However, Lauerward et al.,
367 (2015) found a low negative correlation between them. Abril et al., (2005) noted that intense
368 mineralization of organic matter (OM) originating from the reservoir was possibly a significant source
369 for *p*CO₂ value in downstream river. Thus, the high *p*CO₂ measured at this site may reflect the
370 increased decomposition of OM and/or the water perturbation due to dam construction in this study.

371 4.2 Influence of water discharge and geomorphological characteristics on *p*CO₂ and CO₂ emission

372 *p*CO₂ differences between the three upstream tributaries and the main downstream axe of the Red River
373 are suggested to be partially related to different hydrological characteristics and management of the



374 three sub-basins and delta area, as observed in other systems (Yao et al., 2007; Li et al., 2012). Our
375 results showed that within the 3 upstream sites studied, the highest $p\text{CO}_2$ values were always measured
376 in the Da River at Hoa Binh site, where river discharges were the highest ($2,189 \pm 39 \text{ m}^3 \text{ s}^{-1}$ in wet
377 season and $868 \pm 319 \text{ m}^3 \text{ s}^{-1}$ in dry season), whereas the lowest $p\text{CO}_2$ were measured at the Yen Bai
378 station of the Thao River, where river discharges were the lowest ($840 \pm 68 \text{ m}^3 \text{ s}^{-1}$ in wet season and
379 $260 \pm 18 \text{ m}^3 \text{ s}^{-1}$ in dry season) (Table 1 and Table 2). Figure 7 showed the increased trend of both $p\text{CO}_2$
380 and $f\text{CO}_2$ when river discharge increased in both rainy and dry seasons for the lower Red River.

381 Differences in geomorphological characteristics between the upstream and downstream parts
382 of the lower Red River may be another reason responsible for the variability of $p\text{CO}_2$ observed among
383 the five stations. As presented above, the upstream part of the Red River is located in mountainous
384 areas, where chemical and mechanical erosion are among the world highest (500 mm per 1,000 years)
385 (Meybeck et al., 1989), whereas the downstream part is located in a very flat and low land, with an
386 elevation ranging from 0.4 to 12 m above sea level (Nguyen Ngoc Sinh et al., 1995). Regarding the Ba
387 Lat site, which is situated in the Red River estuary and thus in a very low and flat land, $p\text{CO}_2$ values
388 were lower than in Hanoi. It is interesting to observe that the river water discharge at Hanoi site ($3,296$
389 ± 86 and $1,915 \pm 149 \text{ m}^3 \text{ s}^{-1}$) was about 3 times higher than the one at Ba Lat ($1,269 \pm 93$ and 453 ± 31
390 $\text{m}^3 \text{ s}^{-1}$) in both wet and dry seasons respectively (Table 1), whereas higher $p\text{CO}_2$ values were measured
391 during the dry season in Hanoi than in Ba Lat (1,150 and 800 ppm, respectively), but during the rainy
392 season the values were close, i.e. around 1,450 ppm. We think that dilution by seawater may lead to a
393 reduction of riverine surface water $p\text{CO}_2$, especially in the dry season when the river flow was lower.
394 The higher salinity values measured at Ba Lat site in the dry season (3.6) than in the wet season (0.2)
395 may confirm our suggestion that tidal action influenced at Ba Lat site in the Red River estuary. This
396 result is consistent with previous observations in the Changjiang River estuary (Chen et al., 2008; Bai
397 et al., 2015) or in the Pearl River Estuary (Semiletov et al., 2004; Delille, 2006; Zimmelink et al.,
398 2006).

399

400 **4.3 Influence of population density on $p\text{CO}_2$ and CO_2 emission**

401 From the upstream to the downstream part of the main axe of the lower Red River, $p\text{CO}_2$ increased
402 from Yen Bai (mean value of 995 ppm) to Hanoi (mean value of 1,256 ppm) and then decreased to the
403 estuary at Ba Lat (mean value of 1,154 ppm). Higher values at Hanoi than at Yen Bai may be explained
404 by carbon inputs from the Hanoi wastewater system (Trinh et al., 2007). Indeed, high CO_2 efflux in the
405 peri-urban rivers of the Red River Delta that run through megacity Hanoi, e.g. the Day River (Trinh et
406 al., 2009) and the Nhue River (Trinh et al., 2012) was reported, whereas the upstream zone (Yen Bai) is
407 less subject to anthropogenic pressure. The higher values of both DOC and POC concentrations in
408 Hanoi site than in Yen Bai site may further indicate the influence of organic matter inputs at Hanoi site.

409

410 **4.4. Comparison with World Rivers**

411 CO_2 emissions from the Red River, as determined in the present study, were higher than the ones of
412 some Asian rivers such as the Lupar River ($13 \pm 3.0 \text{ mmol m}^{-2} \text{ d}^{-1}$) and the Saribas River (14.6 ± 3.3
413 $\text{mmol m}^{-2} \text{ d}^{-1}$) in Malaysia (Wit et al., 2015), and much higher than the results from some rivers in



414 Indonesia (Musi, Batanghari, Indragiri, Siak Rivers: 5 ± 1.1 , 1.8 ± 0.4 , 9.7 ± 2.2 , 8.3 ± 1.9 mmol m⁻² d⁻¹,
415 respectively) (Wit et al., 2015) or in upper Yukon River (6 mmol m⁻² d⁻¹) (Striegl et al., 2007).
416 However, CO₂ outgassing from the lower Red River system was found much lower than the ones of
417 many rivers in America and Africa such as the Capibaribe river with 225 mmol m⁻² d⁻¹ (Moacyr et al.,
418 2013), the Amazon river 190 ± 55 mmol m⁻² d⁻¹ (Richey et al., 2002), the Mississippi River (270 mmol
419 m⁻² d⁻¹) (Dubois et al., 2010), some rivers in South America reported by Rasera et al. (2013) such as the
420 Negro, the Solimoes, the Caxiuana rivers (855 ± 294 , 518 ± 17 , 778 ± 17 mmol m⁻² d⁻¹, respectively), or
421 even much lower than the ones of some large Asian rivers as the Yellow river (856 ± 409 mmol m⁻² d⁻¹)
422 (Ran et al., 2015) and the Xijiang river (357 mmol m⁻² d⁻¹) (Yao et al., 2007) (Table 5). Our lower
423 values for the Red River were surprising when considering that large Asian rivers (in Himalayas and
424 Tibet Plateau regions) played important role in terms of chemical weathering (via carbon consumption
425 due to tectonic forcing) (Raymo and Ruddiman, 1992) and carbon burial (France-Lanord and Derry,
426 1997). The present low value of the Red River CO₂ outgassing may be related to the large decrease of
427 suspended solids, associated with strong decrease of particulate organic carbon due to a series of dam
428 construction in the upstream part of the Red River (Le et al., 2017) or due to low water flow in the
429 measured year.

430

431

432 5. Conclusions

433

434 This work presented the estimates of CO₂ emissions at the water-air interface at the 5 sites along the
435 lower Red River system in the dry and rainy seasons. The riverine water *p*CO₂ was supersaturated with
436 CO₂ in contrast to the atmospheric equilibrium (400 ppm), averaging about $1,588.6 \pm 884.6$ ppm, thus
437 resulting in a mean water-air CO₂ flux of 26.9 ± 18.4 mmol m⁻² day⁻¹ from the lower Red River system.
438 The CO₂ outgassing rate from the water surface Red River network was characterized by significant
439 spatial variations, being the highest at the Hoa Binh dam downstream and in the main axe at Hanoi
440 station. The highest value obtained at Hoa Binh site may reflect the important impact of a series of
441 large dams (Son La, Hoa Binh) in the Da river, but also the high water discharge, whereas the high
442 *p*CO₂ value in Hanoi may reflect the influence of population density, notably through the release of
443 elevated amount of organic carbon into the river. The monsoon season resulted in an increased amount
444 of OM inputs from adjacent soil, and combined to an increase of temperature, led to higher *p*CO₂
445 values. During the dry season, temperature appeared to be the main factor controlling *p*CO₂. Regarding
446 CO₂ evasion, differences appeared between the day and night in both dry and rainy seasons at almost
447 all sites with higher values found in the day time (30.4 ± 21.2 mmol m⁻² day⁻¹) than in the night time
448 (23.3 ± 15.4 mmol m⁻² day⁻¹). This result was related to the combined higher wind speed and higher
449 temperatures during the day. Consequently, this study evidenced that CO₂ dynamic along the lower
450 Red River was controlled by both anthropogenic activities (dam, urban effluents), and natural
451 meteorological-hydrological characteristics (rainfall- river discharge and temperature).

452 Author contribution



453 Le TPQ, Marchand C and Ho TC designed the experiments. Le TPQ, Ho TC and Vu DA carried the in-
454 situ experiments. Phuong KD and Le ND contribute to data treatment and calculations. Le TPQ and
455 Marchand C prepared the manuscript with the contributions from all co-authors.

456 Acknowledgements

457 This work was performed in the framework of the *ARCP2014-03CMY-QuyNh/ARCP2013-06CMY-*
458 *QuyNh/ARCP2012-11MY-QuyNh* and the *Vietnam-NAFOSTED 105.09-2012.10* projects. The authors
459 would like to thank and the Asia-Pacific Network for Global Change Research (APN) and the
460 Vietnam's National Foundation for Science and Technology Development (NAFOSTED-Vietnam) for
461 their financial supports. We thank Ms Nguyen Bich Ngoc and Mr Nguyen Trung Kien for helping field
462 work.

463 References

- 464 Abril, G., and Borges, A. V.: Carbon dioxide and methane emissions from estuaries, In Greenhouse
465 gases emissions from natural environments and hydroelectric reservoirs: Fluxes and processes,
466 Edited by A. Tremblay, L. Varfalvy, C. Roehm, and M. Garneau, pp. 187–207, Springer, Berlin,
467 Germany, 2004.
- 468 Abril, G., Etcheber, H., Borges, A. V., and Frankignoulle, M.: Excess atmospheric carbon dioxide
469 transported by rivers into the Scheldt estuary, *Earth Planet Sci.*, 330(11), 761–768, 2000.
- 470 Abril, G., Guérin, F., Richard, S., Delmas, R., Galy-Lacaux, C., Gosse, P., Tremblay, A., Varfalvy, L.,
471 Dos Santos, M.A, and Matvienko, B.: Carbon dioxide and methane emissions and the carbon
472 budget of a 10-year old tropical reservoir (Petit Saut, French Guiana), *Global Biogeochem. Cycle*.
473 19, GB4007, doi:10.1029/2005GB002457, 2005.
- 474 Abril, G., Commarieu, M V., Sottolichio, A., Bretel, P., and Guerin, F.: Turbidity limits gas exchange
475 in a large macrotidal estuary, *Estuar. Coast. Shelf. Sci.*, 83, 342–348,
476 doi:10.1016/j.ecss.2009.03.006, 2009.
- 477 Abril, G., Bouillon, S., Darchambeau, F., Teodoru, C. R., Marwick, T. R., Tamoo, F., Ochieng F.,
478 Omengo, F., Geeraert, N., Deirmendjian, L., Polsenaere, P., and Borges, A.V.: Technical Note:
479 Large overestimation of pCO₂ calculated from pH and alkalinity in acidic, organic-rich
480 freshwaters, *Biogeosciences*, 12, 67-78, doi:10.5194/bg-12-67-2015, 2015.
- 481 Alin, S. R., Fatima, R. M., Salimon, C.I., Richey, J. E., Krusche, A. V., Holtgrieve G. W., and
482 Snidvongs, A.: Physical controls on carbon dioxide transfer velocity and flux in low-gradient river
483 systems and implications for regional carbon budgets, *J. Geophys. Res.* 116, G0100, 2011.
- 484 Amorocho, J. and DeVries, J.J.: A new evaluation of the wind stress coefficient over water surfaces, *J*
485 *Geophys Res.*, 85, 433–442, 1980.
- 486 APHA, (American Public Health Association). : Standard Methods for the Examination of Water and
487 Wastewater, American Public Health Association editor, 1995.



- 488 Appendix 8.6 wind speed calculations. : Partnerships For Renewables, HMP Standford Hill Wind
489 Energy Development, p 1- 4, 2010.
- 490 Battin, T. J., Luysaert, S., Kaplan, L. A., Aufdenkampe, A. K., Richter, A., and Tranvik, L. J.: The
491 boundless carbon cycle, *Nat. Geosci.*, 2, 598-600, 2009.
- 492 Bauer, J. E., Cai, W.-J., Raymond, P. A., Bianchi, T. S., Hopkinson, C.S. and Regnier, P.A.G.: The
493 changing carbon cycle of the coastal ocean, *Nature*, 504(7478), 61–70, doi:10.1038/nature12857,
494 2013.
- 495 Borges, A.V., Djenidi, S., Lacroix, G., Theate, J., Delille B., and Frankignoulle, M.: Atmospheric CO₂
496 flux from mangrove surrounding waters, *Geophys. Res. Lett.*, 30(11), 1558, 2003.
- 497 Bai, Y., Cai, W.-J., He, X., Zhai, W., Pan, D., Dai, M., and Yu, P.: A mechanistic semi-analytical
498 method for remotely sensing sea surface pCO₂ in river-dominated coastal oceans: A case study
499 from the East China Sea, *J. Geophys. Res. Oceans*, 120, 2331– 2349, doi:10.1002/2014JC010632,
500 2015.
- 501 Cai, W.J., Guo, X., Chen, C-T. A., Dai, M., Zhang, L., Zhai, W., Lohrenz, S., Yin, K., Harrison P. and
502 Wang, Y.: A comparative overview of weathering intensity and HCO₃⁻ flux in the world's major
503 rivers with emphasis on the Changjiang, Huanghe, Zhujiang (Pearl) and Mississippi Rivers, *Cont.*
504 *Shelf. Res.*, 28, 1538-1549, 2008.
- 505 Carini, S., Weston, N., Hopkinson, C., Tucker, J., Gilbin, A., and Vallino, J.: Gas exchange in the
506 Parker estuary, MA. *Biol. Bull.* 191: 333-334, 1996.
- 507 Clark, J. F., Shlosser, P., Simpson, H. J., Stute, R., Wanninkhof, R. and Ho, D.T.: Relationship between
508 gas transfer velocities and wind speeds in the tidal Hudson River determined by the dual tracer
509 technique, In *Air-Water Gas Transfer*, edited by B.Jahne and E.Monahan, pp. 175-800, Aeon
510 Verlag, Hanau, 1995.
- 511 Cole, J. J. and Caraco, N. F.: Atmospheric exchange of carbon dioxide in a low-wind oligotrophic lake
512 measured by the addition of SF₆, *Limnol. Oceanogr.* 43, 647-656, 1998.
- 513 Cole, J. J., and Caraco, N.F.: Carbon in catchments: connecting terrestrial carbon losses with aquatic
514 metabolism, *J. Mar. Freshwater Res.*, 52(1), 101 – 110, 2001.
- 515 Cole, J. J., Pace, M. L., Carpenter, S. R., and Kitchell, J. F.: Persistence of net heterotrophy in lakes
516 during nutrient addition and food web manipulations, *Limnol. Oceanogr.*, 45(8), 1718–1730.
517 DOI: 10.4319/lm.2000.45.8.1718, 2000.
- 518 Chanda, A., Akhand, A., Manna, S., Dutta, S., Hazra, S, Das, I., and Dadhwal, V. K.: Characterizing
519 spatial and seasonal variability of carbon dioxide and water vapour fluxes above a tropical mixed
520 mangrove forest canopy, India. *J. Earth Syst. Sci.*, 122(2), 503–513, 2013.
- 521 Chen, C.T.A., Zhai, W.D., and Dai, M.: Riverine input and air–sea CO₂ exchanges near the
522 Changjiang (Yangtze River) Estuary: Status quo and implication on possible future changes in
523 metabolic status, *Cont. Shelf Res.*, 28, 1476–1482, 2008.



- 524 Dang, T.H., Coynel, A., Orange, D., Blanc, G., Etcheber, H., and Le, L.A.: Long-term monitoring
525 (1960–2008) of the river-sediment transport in the Red River Watershed (Vietnam): Temporal
526 variability and dam-reservoir impact, *Sci Total Environ.*, 408, 4654–4664, 2010.
- 527 Dessert, C., Dupré, B., Gaillardet, J., Francois, L. M., and Allegre, C.J.: Basalt weathering laws and the
528 impact of basalt weathering on the global carbon cycle. *Chem. Geol.*, 202, 257–273, 2003.
- 529 Devol, A.H., Quay, P.E., Richey, J.E., and Martinelli, L.A.: The role of gas exchange in the inorganic
530 carbon, oxygen, and ²²²Rn budgets of the Amazon River, *Limnol Oceanogr*, 32, 235-248, 1987.
- 531 Dornblaser, M. and Striegl, R.: Seasonal variation in diel carbon dynamics, Beaver Creek, Alaska,
532 AGU Fall Meeting Abstracts, p 15–27, 2013.
- 533 Dubois, K. D., Lee, D., and Veizer, J.: Isotopic constraints on alkalinity, dissolved organic carbon,
534 and atmospheric carbon dioxide fluxes in the Mississippi River, *J. Geophys. Res.*, 115, G02018,
535 doi:10.1029/2009JG001102, 2010.
- 536 Delille, B.: Inorganic carbon dynamics and air-sea CO₂ fluxes in the open and coastal waters of the
537 Southern Ocean, Ph. D. thesis, Univ. of Liège, Liège, Belgium, 1–297, 2006.
- 538 Frankignoulle, M., Borges, A., and Biondo, R.: A new design of equilibrator to monitor carbon dioxide
539 in highly dynamic and turbid environments, *Wat. Res.* 35(5), 1344–1347, 2001.
- 540 France-Lanord, C. and Derry, L.A.: Organic carbon burial forcing of the carbon cycle from Himalayan
541 erosion, *Nature*, 390(6), 65-67. DOI: 10.1038/36324, 1997.
- 542 Fullen, M. A., Mitchell, D. J., Barton, A. P., Hocking, T. J., Liguang, L., Zhi, W. B., Yi, Z., and Yuan,
543 X.Z.: Soil erosion and Conservation in the Headwaters of the Yangtze River, Yunnan Province,
544 China, In *Headwaters: Water resources and Soil conservation*, edited by Haigh MJ, Kreckel J,
545 Rajwar S, Kilmartin MP, pp. 299–306, Balkema, Rotterdam/Oxford and IBH, New Delhi, 460pp,
546 1998.
- 547 Guasch, H., Armengol, J. and Sabater, S.: Diurnal variation in dissolved oxygen and carbon dioxide in
548 two low-order streams, *Water Res.*, 32,1067–1074, 1998.
- 549 Guérin, F., Abril, G., Serça, D., Delon, C., Richard, S., Delmas, R., Tremblay, A., and Varfalvy, L.:
550 Gas transfer velocities of CO₂ and CH₄ in a tropical reservoir and its river downstream, *J. Mar.*
551 *Syst.*, 66, 161–172, 2007.
- 552 Hope, D., Palmer, S.M., Billett, M.F., and Dawson, J.J.: Variations in dissolved CO and CH₄ in a first-
553 order stream and catchment: an investigation of soil-stream linkages, *Hydrol. Process.*, 18, 3255–
554 75, 2004.
- 555 Ho, D. T., Coffineau, N., Hickman, B., Chow, N., Koffman, T., and Schlosser, P.: Influence of current
556 velocity and wind speed on air-water gas exchange in a mangrove estuary, *Geophys. Res. Lett.*, 43,
557 3813–3821, doi:10.1002/2016GL068727, 2016.
- 558 Jähne, B., Huber, W., Dutzi, A., Wais, T., and Ilmberger, J.: Wind/wave-tunnel experiments on the
559 Schmidt number and wave field dependence of air-water gas exchange, In *Gas Transfer at Water*
560 *Surfaces*, Ed. W. Brutsaert, G.H. Jirka, pp. 303–309, Riedel, Hingham, MA, 1984.



- 561 Lauerwald, R., Laruelle, G. G., Hartmann, J., Ciais, P., and Regnier, P. A. G.: Spatial patterns in
562 CO₂ evasion from the global river network, *Global Biogeochem. Cy.*, 29(5), 534–554,
563 DOI: 10.1002/2014GB004941, 2015.
- 564 Leopold, A., Marchand, C., Deborde, J., and Allenbach, M.: Biogeochemistry of an estuary surrounded
565 by mangroves under semi-arid climate (New Caledonia), *Estuaries and Coasts*, 40, 3, 773–791,
566 2017.
- 567 Le, T. P. Q., Garnier, J., Billen, G., Thery, S., and Chau, V.M.: The changing flow regime and
568 sediment load of the Red River, Viet Nam, *J. Hydrol.*, 334, 199– 214,
569 doi:10.1016/j.jhydrol.2006.10.020, 2007.
- 570 Le, T. P. Q., Billen, G., Garnier, J., Chau, V. M.: Long-term biogeochemical functioning of the Red
571 River (Vietnam): past and present situations, *Reg. Environ. Change.*, DOI: 10.1007/s10113-014-
572 0646-4, 2015.
- 573 Le, T. P. Q., Dao, V. N., Rochelle-Newall, E., Garnier, J., Billen, G., Lu, X. X., Echetbet, H., Duong,
574 T. T., Ho, C. T., Nguyen, T. B. N., Nguyen, B. T., Nguyen, T. M. H., Le, N. D., and Pham, Q. L.:
575 Total organic flux of the Red River system (Vietnam), *Earth. Surf. Proc. Land.*,
576 DOI: 10.1002/esp.4107, 2017.
- 577 Liss, P.S. and Merlivat, L.: Air-sea gas exchange rates: introduction and synthesis. In *The Role of Air-
578 Sea Exchange in Geochemical Cycling*, ed. P Buat-Menard, 113–129, Reidel publishing company,
579 Boston, 1986.
- 580 Li, S., Lu, X. X., He, M., Yue, Z., Li L., and Ziegler, A. D.: Daily CO₂ partial pressure and CO₂
581 outgassing in the upper Yangtze River basin: A case study of the Longchuan River, China, *J.
582 Hydrol.*, 466–467, 141–150, <http://dx.doi.org/10.1016/j.jhydrol.2012.08.011>, 2012.
- 583 Li, S., Lu, X. X., and Bush, R. T.: CO₂ partial pressure and CO₂ emission in the Lower Mekong River,
584 *J. Hydrol.*, 504, 40–56, <http://dx.doi.org/10.1016/j.jhydrol.2013.09.024>, 2013.
- 585 Linn, D. M. and Doran, J. W.: Effect of water-filled pore space on carbon dioxide and nitrous oxide
586 production in tilled and non- tilled soils, *Soil Sci. Soc.* 48(6), 1267–272, 1984.
- 587 Lu, X. X.: Vulnerability of water discharge of large Chinese rivers to environmental changes: an
588 overview, *Reg. Environ. Change*, 4, 182–191, 2004.
- 589 Lu, X. X., Oeurng, C., Le T. P. Q., and Duong T. T.: Sediment budget as affected by construction of a
590 sequence of dams in the lower Red River, Viet Nam. *Geomorphology* 248, 125–133, 2015.
- 591 Marino, R., and Howarth, R.W.: Atmospheric oxygen exchange in the Hudson River: Dome
592 measurements and comparison with other natural waters, *Estuaries*, 16, 433–445, 1993.
- 593 Meybeck, M., Chapman, D. V. and Helmer, R.: *Global freshwater quality: a first assessment.*
594 Cambridge, MA, World Health Organization/United Nations Environment Programme, Basil
595 Blackwell, Inc. 306 p, 1989.



- 596 Melack, J. M. and Engle, D. L.: An organic carbon budget for an Amazon floodplain lake, *Verh. Int.*
597 *Ver. Limnol.*, 30, 1179–1182, 2009.
- 598 Moacyr, A., Carlos, N., Doris, V., and Nathalie, L.: Nutrient input and CO₂ flux of a tropical coastal
599 fluvial system with high population density in the northeast region of Brazil, *J. Water Resource*
600 *Prot.*, 5, 362-375, 2013.
- 601 MONRE.: Vietnamese Ministry of Environment and Natural Resources, Report Annual on
602 Hydrological Observation in Vietnam, Hanoi, 2016.
- 603 Nguyen, N. S., Hua, C. T., Nguyen, C. H., Nguyen, V. T., Lang, V. K., Pham, V. N., and Nguyen, V.
604 T.: Case study report on Red River Delta in Vietnam - Project on integrated management and
605 conservation of near shore coastal and marine areas in East Asia region (EAS-35) United Nations
606 Environment program, Regional coordinating for the East Seas (ESA/RCU), U.N. Environ.
607 Programme, Nairobi, 78pp, 1995.
- 608 Nomura, D., Yoshikawa-Inoue, H., Kobayashi, S., Nakaoka, S., Nakata, K., and Hashida, G.: Winter-
609 to-summer evolution of pCO₂ in surface water and air–sea CO₂ flux in the seasonal ice zone of the
610 Southern Ocean, *Biogeosciences*, 11, 5749–5761, doi:10.5194/bg-11-5749-2014, 2014.
- 611 Parkin, T. B. and Kaspar, T. C.: Temperature controls on diurnal carbon dioxide flux, *Soil Sci. Soc.*
612 *Am. J.*, 67, 1763–1772, 2003.
- 613 Peter, H., Singer, G. A., Preiler, C., Chiffard, P., Steniczka, G., and Battin, T. J.: Scales and drivers of
614 temporal pCO₂ dynamics in an Alpine stream. *J. Geophys. Res. Biogeosciences*, 119 (6), 1078–
615 1091, doi 10.1002/2013JG002552, 2014.
- 616 Patricia, S., Raymond, H. H., and Kelly, C.A.: Continuous measurement of CO₂ for estimation of air-
617 water fluxes in lakes: An in situ technique, *Limnol. Oceanogr.*, 40(3), 575-581, 1995.
- 618 Roulet, N. T., Crill, P., Comer, N., Dove, A., and Boubonniere, R.: CO₂ and CH₄ flux between a boreal
619 beaver pond and the atmosphere, *J. Geophys. Res. D*, 102, 29313–29319, 1997.
- 620 Ran, L., Lu, X. X., Richey, J. E., Sun, H., Han, J., Yu, R., Liao, S., and Yi, Q.: Long term spatial and
621 temporal variation of CO₂ partial pressure in the Yellow River, China, *Biogeosciences*, 12, 921-
622 932, DOI: 10.5194/bg-12-921-2015, 2015.
- 623 R Core Team. R.: A language and environment for statistical computing. Vienna, Austria: R
624 Foundation for Statistical Computing, Retrieved from <https://www.rproject.org/>, 2016.
- 625 Rasera M de Fatima, F.L., Krusche, A.V., Richey, J. E., Ballester, M. V. R., and Victória, R. L.: Spatial
626 and temporal variability of pCO₂ and CO₂ efflux in seven Amazonian Rivers, *Biogeochem.*,
627 116:241–259, doi: 10.1007/s10533-013-9854-0, 2013.
- 628 Raymond, M. E., and Ruddiman, W. F.: Tectonic forcing of late Cenozoic climate, *Nature*, 359, 117-
629 122, 1992.
- 630 Raymond, P. A., and Cole, J. J.: Gas Exchange in Rivers and Estuaries: Choosing a Gas Transfer
631 Velocity, *Estuaries*, 24(2), 312-317, doi:10.2307/1352954, 2001.



- 632 Raymond, P. A., Caraco, N. F. and Cole, J. J.: Carbon dioxide concentration and atmospheric flux in
633 the Hudson River, *Estuaries*, 20, 381–390, 1997.
- 634 Raymond, P. A., Zappa, C. J., Butman, D., Bott, T. L., Potter, J., Mulholland, P., Laursen, A. E.,
635 McDowell, W.H., and Newbold, D.: Scaling the gas transfer velocity and hydraulic geom-etry in
636 streams and small rivers, *Limnol. Oceanogr.*, 2, 41–53, doi:10.1215/21573689-1597669, 2012.
- 637 Raymond, P. A., et al. : Global carbon dioxide emissions from inland waters, *Nature*, 503(7476), 355–
638 359. Doi:10.1038/nature12760, 2013.
- 639 Regnier, P., Friedlingstein, P., Ciais, P., Mackenzie, F. T., Gruber, N., Janssens, I. A., Laruelle, G. G.,
640 Lauerwald, R., Luysaert, S., Andersson, A. J., Arndt, S., Arnosti, C., Borges, A. V., and Dale,
641 A.W.: Anthropogenic perturbation of the carbon fluxes from land to ocean, *Nat. Geosci.*, 6(8),
642 597–607, doi:10.1038/ngeo1830, 2013.
- 643 Rey, A., Beilelli-Marchesini, L., Were, A., Serrano-Ortiz, P., Etiopie, G., Papale, D., Domingo, F., and
644 Pegoraro, E.: Wind as a main driver of the net ecosystem carbon balance of a semiarid
645 Mediterranean steppe in the South East of Spain, *Glob. Change Biol.*, 18, 539–554, doi:
646 10.1111/j.1365-2486.2011.02534.x, 2012.
- 647 Richey, J. E., Melack, J. M., Aufdenkampe, A. K., Ballester, V. M., and Hess, L. L.: Outgassing from
648 Amazonian rivers and wetlands as a large tropical source of atmospheric CO₂, *Nature*, 416, 617–
649 620, 2002.
- 650 Roulet, N. T., Crill, P., Comer, N., Dove, A., and Boubonniere, R.: CO₂ and CH₄ flux between a boreal
651 beaver pond and the atmosphere, *J. Geophys. Res. D*, 102, 29313–29319, 1997.
- 652 Rudorff, C. M., Melack, J. M., Sally, M., Cláudio, C. F. B., and Evlyn, M. L. M. N.: Seasonal and
653 spatial variability of CO₂ emission from a large floodplain lake in the lower Amazon, *J. Geophys.*
654 *Res.*, 116, G04007, doi:10.1029/2011JG001699, 2011,
- 655 Semiletov, I., Makshtas, S., Akasofu, S., and Andreas, E. L.: Atmospheric CO₂ balance: The role of
656 Arctic sea ice, *Geophys. Res. Lett.*, 31(5), doi:10.1029/2003GL017996, 2004.
- 657 Servais, P., Barillier, A., and Garnier, J.: Determination of the biodegradable fraction of dissolved and
658 particulate organic carbon in waters. *Int. J. Limnol.* 31(1):75-80. Doi:10.1051/limn/1995005, 1995.
- 659 Striegl, R. G., Dornblaser, M. M., Aiken, G. R., Wickland, K. P., and Raymond, P. A.: Carbon export
660 and cycling by the Yukon, Tanana, and Porcupine rivers, Alaska, 2001–2005, *Water Resour. Res.*,
661 43, W02411, doi:10.1029/2006WR005201, 2007.
- 662 Striegl, R. G., Dornblaser, M. M., McDonald, C. P., Rover, J. R., and Stets, E. G.: Carbon dioxide and
663 methane emissions from the Yukon River system, *Global Biogeochem. Cy.*, 26, GB0E05,
664 doi:10.1029/2012GB004306, 2012.
- 665 Sun, H. G., Han, J., Lu, X. X., Zhang, S. R., and Li, D.: An assessment of the riverine carbon flux of
666 the Xijiang River during the past 50 years, *Quatern. Int.*, 226, 38-43, 2010.



- 667 Tranvik, L. J., Downing, J. A., Cotner, J. B., Loiselle, S. A., Striegl, R. G., Ballatore, T. J., Dillon, P.,
668 Finlay, K., Fortino, K., Knoll, L.B., Kortelainen, P.L.: Lakes and reservoirs as regulators of carbon
669 cycling and climate. *Limnol. Oceanogr.*, 54 (6, part 2), 2298–2314, 2009.
- 670 Trinh, A. D., Vachaud, G., Bonnet, M. P., Prieur, N., Vu, D. L., and Le, L. A.: Experimental
671 investigation and modelling approach of the impact of urban wastewater on a tropical river; a case
672 study of the Nhue River, Hanoi, Vietnam, *J. Hydrol.*, 334, 347–358, doi:10.1016/j.
673 jhydrol.2006.10.022, 2007.
- 674 Trinh, A. D., Giang, N. H., Vachaud, G., and Choi, S.U.: Application of excess carbon dioxide partial
675 pressure (EpCO₂) to the assessment of trophic state of surface water in the Red River Delta of
676 Vietnam, *Int. J. Environ. Stud.*, 66(1), 27–47, doi:10.1080/00207230902760473, 2009.
- 677 Trinh, A.D., Meysman, F., Rochelle-Newall E., and Bonnet, M. P.: Quantification of sediment-water
678 interactions in a polluted tropical river through biogeochemical modeling, *Global Biogeochem*
679 *Cy.*, 26, GB3010, doi:10.1029/2010GB003963, 2012.
- 680 Takahashi, T., Sutherland, S.C., Sweeney, C., Poisson, A., Metzl, N., Tilbrook, B., Bates, N.,
681 Wanninkhof, R., Feely, R. A., Sabine, C., Olafsson, J., and Nojiri, Y.: Global air-sea CO₂ flux
682 based on climatological surface ocean pCO₂ and seasonal biological and temperature effects,
683 *Deep-Sea Res.*, 49, 1601–1622, 2002.
- 684 Vachon, D., Prairie, Y.T., and Cole, J.J.: The relationship between near-surface turbulence and gas
685 transfer velocity in freshwater systems and its implications for floating chamber measurements of
686 gas exchange, *Limnol. Ocean.*, 55, 1723–1732, 2010.
- 687 Xu, J., Lee, X., Xiao, W., Cao, C., Liu, S., Wen, X., Xu, J., Zhang, Z., and Zhao, J.: Interpreting the
688 ¹³C= ¹²C ratio of carbon dioxide in an urban airshed in the Yangtze River Delta, China, *Atmos.*
689 *Chem. Phys.*, 17, 3385–3399, doi:10.5194/acp-17-3385-2017, 2017.
- 690 Yao, G., Quanzhou, G., Zhengang, W., Xiakun, H., Tong, H., Yongling, Z., Shulin, J., and Jian, D.:
691 Dynamics of CO₂ partial pressure and CO₂ outgassing in the lower reaches of the Xijiang River, a
692 subtropical monsoon river in China, *Sci. Total Environ.*, 376, 255–266. DOI:
693 10.1016/j.scitotenv.2007.01.080, 2007.
- 694 Walling, D. E., and Fang, D.: Recent trends in the suspended sediment loads of the world's rivers,
695 *Glob. Planet. Change*, 39(1-2), 111-126, 2003.
- 696 Walling, D. E.: Human impact on land-ocean sediment transfer by the world's rivers, *Geomorphology*,
697 79(3-4), 192-216, 2006.
- 698 Wang, F., Wang, Y., Zhang, J., Xu, H., and Wei, X.: Human impact on the historical change of CO₂
699 degassing flux in the River Changjiang, *Chem. Trans.*, Doi:10.1186/1467-4866-8-7, 2007.
- 700 Wang, Y., Munger, J. W., Xu, S., McElroy, M. B., Hao, J., Nielsen, C. P. and Ma, H.: CO₂ and its
701 correlation with CO at a rural site near Beijing: implications for combustion efficiency in China,
702 *Atmos. Chem. Phys.*, 10, 8881–8897, doi:10.5194/acp-10-8881-2010, 2010.



- 703 Wang, F., Wang, B., Liu, C., Wang, Y., Guan, J., Liu, X., and Yu, Y.: Carbon dioxide emission from
704 surface water in cascade reservoirs-river system on the Maotiao River, southwest of China, Atmos.
705 Environ., 45(23), 3827–3834, 2011.
- 706 Weiss, R. F.: Carbon dioxide in water and seawater: the solubility of a non ideal gas, Mar. Chem., 2(3),
707 203-215, 1974.
- 708 Wit, F., Muller, D., Baum, A., Warneke, T., Pranowo, W. S., Muller, M. and Rixen T.: The impact of
709 disturbed peatlands on river outgassing in Southeast Asia, Nat. Commun. 6:10155, DOI:
710 10.1038/ncomms10155, 2015.
- 711 Zimmelink, H. J ., Delille, B., Tison, J. L., Hintsa, E. J., Houghton, L. and Dacey, J. W. H.: CO₂
712 deposition over the multi-year ice of the western Weddell Sea, Geophys. Res. Lett., 33, L13606,
713 doi:10.1029/2006GL026320, 2006.
- 714
- 715



716 **List of tables**

717 **Table 1.** Average values of river water discharge at five hydrological stations of the Red River in 2014

718 **Table 2.** Mean values of the different physico-chemical variables at 5 sites in wet and dry season in
719 2014.

720 **Table 3.** Wind speed, k_{600} parameterization, and calculated water-air CO₂ fluxes for day and night at
721 five hydrological stations of the Red River in dry and wet seasons in 2014.

722 **Table 4.** Summary of the statistical analysis at Hanoi station with the environmental variables.

723 **Table 5.** CO₂ out-gassing flux from some World Rivers.

724

725

726



Table 1. Average values of river water discharge at five hydrological stations of the Red River in 2014.

Hydrological stations	Altitude (m a.s.l.)	Latitude	Average daily water discharge in 2014, $\text{m}^3 \text{s}^{-1}$	Water discharge, $\text{m}^3 \text{s}^{-1}$			
				<i>Wet season</i>		<i>Dry season</i>	
				Mean value in wet season in 2014 (May – Oct)	On the date of measurement Sept 2014	Mean value in wet season in 2014 (May – Oct)	On the date of measurement in Nov 2014
Yen Bai	56	104°51' - 21°42'	527 ± 515	788 ± 459	840 ± 68	262 ± 530	260 ± 18
Hoa Binh	23	105°19' - 20°49'	1,369 ± 833	1,907 ± 451	2,189 ± 39	825 ± 515	868 ± 319
Vu Quang	25	105°15' - 21°34'	1,302 ± 517	1,618 ± 378	2,240 ± 88	982 ± 284	725 ± 11
Hanoi	5	105°51' - 21°01'	1,867 ± 1089	2,598 ± 780	3,296 ± 86	1,127 ± 490	1,915 ± 149
Ba Lat	0	106°00' - 19°30'	615 ± 293	824 ± 200	1,269 ± 93	403 ± 96	453 ± 31


Table 2. Average values in day and night times of the different physico-chemical variables at 5 sites in wet and dry seasons in 2014.

Stations	Temperature °C	pH	TAlk mg L ⁻¹	Salinity	Chl-a µg L ⁻¹	Turbidity NTU	Conductivity mS cm ⁻¹	DOC mg L ⁻¹	POC mg L ⁻¹	DO %	Measured pCO ₂ ppm	Calculated pCO ₂ ppm
Wet season												
<i>1-Yen Bai</i>												
Day	26.4±0.1	8.2±0.1	105.1±5.2	0.1±0.0	3.1±0.1	141.6±8.6	0.2±0.0	1.5±0.2	2.1±0.4	69.9±0.2	964.3±9.9	269.6±36.4
Night	26.6±0.0	8.3±0.0	103.8±3.3	0.1±0.0	3.1±0.1	135.4±4.0	0.2±0.0	1.4±0.2	1.9±0.2	70.4±0.1	979.5±9.6	225.7±10.4
<i>2-Vu Quang</i>												
Day	26.8±0.1	8.1±0.0	148.9±6.7	0.1±0.0	1.2±0.2	51.4±7.5	0.2±0.0	1.1±0.3	1.4±0.2	63.6±1.2	1598.7±53.3	453.8±55.2
Night	27.0±0.1	8.2±0.0	144.9±3.3	0.1±0.0	1.2±0.2	49.9±5.3	0.2±0.0	1.0±0.2	1.4±0.2	63.2±0.7	1583.0±36.6	404.0±12.5
<i>3-Hoa Binh</i>												
Day	26.5±0.1	7.8±0.0	110.4±3.3	0.1±0.0	0.8±0.3	42.5±4.7	0.2±0.0	1.5±0.4	1.1±0.2	54.9±0.2	3827.1±60.6	881.1±123.0
Night	26.4±0.0	7.8±0.0	107.8±5.4	0.1±0.0	1.2±0.0	41.0±0.1	0.2±0.0	1.3±0.2	1.1±0.1	55.1±0.6	3830.2±19.1	722.0±23.4
<i>4-Ha Noi</i>												
Day	28.6±0.2	8.0±0.0	84.3±1.9	0.1±0.0	2.0±0.6	88.9±1.3	0.2±0.0	4.7±0.6	2.0±0.3	64.0±0.4	1412.3±4.2	336.6±38.6
Night	28.6±0.2	8.1±0.0	84.5±1.5	0.1±0.0	2.7±0.1	88.5±2.7	0.2±0.0	4.2±0.9	2.2±0.4	63.5±0.3	1411.4±6.7	279.4±18.7
<i>5-Ba Lat</i>												
Day	28.9±0.4	8.0±0.1	116.4±4.6	0.3±0.3	1.8±0.3	47.7±8.8	0.6±0.6	1.5±0.4	1.1±0.4	66.1±1.4	1489.1±104.2	495.4±108.6
Night	28.8±0.3	8.1±0.0	114.9±3.5	0.1±0.1	2.5±0.1	81.3±10.0	0.3±0.2	1.7±0.5	1.5±0.2	65.1±1.6	1483.1±117.5	430.2±31.8
Dry season												



<i>1-Yen Bai</i>												
Day	24.1±0.5	8.1±0.1	113.9±7.9	0.1±0.0	1.2±0.3	49.3±7.9	0.2±0.0	1.3±0.3	1.4±0.1	69.3±0.7	995.8±17.5	376.6±140.1
Night	24.2±0.3	8.2±0.0	109.3±2.8	0.1±0.0	1.6±0.2	42.5±4.7	0.2±0.0	1.2±0.2	1.2±0.3	69.1±0.5	1030.6±21.5	266.6±7.8
<i>2-Vu Quang</i>												
Day	24.7±0.2	8.3±0.0	134.9±5.1	0.1±0.0	1.0±0.2	28.1±1.7	0.2±0.0	1.1±0.2	1.1±0.2	67.0±0.9	1235.3±76.2	301.8±36.4
Night	24.8±0.4	8.4±0.0	129.3±2.7	0.1±0.0	1.4±0.2	32.4±3.7	0.2±0.0	1.1±0.2	1.2±0.1	69.0±0.9	1163.3±86.3	235.2±13.0
<i>3-Hoa Binh</i>												
Day	26.3±0.0	7.8±0.0	122.5±6.1	0.1±0.0	0.5±0.1	16.9±0.3	0.2±0.0	0.9±0.2	1.0±0.2	51.5±0.4	2399.3±33.6	869.7±96.9
Night	26.3±0.0	7.8±0.0	120.6±6.1	0.1±0.0	0.5±0.1	17.1±0.5	0.2±0.0	0.9±0.2	1.1±0.2	51.3±0.2	2458.9±14.0	833.1±85.3
<i>4-Ha Noi</i>												
Day	23.8±0.1	8.2±0.0	123.5±2.4	0.1±0.0	1.7±0.2	65.2±1.8	0.2±0.0	2.7±0.7	1.5±0.3	66.8±0.4	1141.3±33.5	333.5±43.2
Night	23.8±0.1	8.3±0.0	123.8±1.5	0.1±0.0	1.6±0.1	62.6±0.7	0.2±0.0	2.0±0.7	1.3±0.1	67.1±0.3	1136.0±24.2	300.6 ± 12.6
<i>5-Ba Lat</i>												
Day	23.7±0.1	8.3±0.0	152.9±6.6	3.9±2.4	1.8±0.2	34.1±8.3	6.6±3.4	1.4±0.2	2.0±0.4	70.0±0.5	751.4±49.3	311.8± 20.5
Night	23.4±0.1	8.3±0.0	150.3±5.6	3.3±1.6	1.3±0.2	28.8±4.2	5.7±2.6	1.2±0.2	1.9±0.4	68.8±0.6	881.0±88.4	331.6± 20.4



Table 3. Wind speed, k_{600} parameterization, and calculated water-air CO_2 fluxes for daytime and nighttime at five hydrological stations of the Red River in dry and wet seasons in 2014.

	Wind speed m s^{-1}	k_{600} cm h^{-1}	Water-air CO_2 flux $\text{mmol m}^{-2} \text{d}^{-1}$	
			With $p\text{CO}_2$ measured from equilibrator	With $p\text{CO}_2$ calculated from $\text{CO}_2\text{-SYS}$
Wet season				
Yen Bai				
Day	1.1±0.6	2.9±0.6	13.0±2.7	7.2±2.3
Night	0.5±0.6	2.3±0.5	10.9±2.5	4.0±1.0
Vu Quang				
Day	0.9±0.7	2.7±0.7	27.7±7.3	16.8±5.6
Night	0.4±0.6	2.3±0.5	20.4±3.9	12.2±2.9
Hoa Binh				
Day	1.3±1.1	3.3±1.2	82.7±36.3	48.4±23.4
Night	0.2±0.5	2.1±0.5	61.3±15.3	23.1±4.3
Hanoi				
Day	1.8±0.7	3.6±0.8	29.4±7.1	15.0±4.6
Night	1.2±0.6	2.9±0.6	24.8±4.6	8.7±2.8
Ba Lat				
Day	0.5±0.5	2.3±0.5	19.0±2.3	17.9±7.8
Night	0.2±0.3	2.0±0.3	18.1±4.0	12.7±2.5
Dry season				
1-Yen Bai				
Day	1.4±0.9	3.2±1.0	14.4±3.7	12.0±7.1
Night	0.5±0.8	2.4±0.8	12.5±4.7	4.9±1.7
2-Vu Quang				
Day	1.3±0.6	3.1±0.6	20.3±5.1	8.9±3.1
Night	0.7±1.3	2.8±1.5	15.8±8.0	4.4±2.0
3- Hoa Binh				
Day	1.2±0.8	3.0±0.8	50.2±13.6	40.3±8.9
Night	0.5±0.5	2.3±0.5	37.2±6.9	29.8±4.8
4-Hanoi				
Day	2.4±0.5	4.6±0.9	28.5±5.8	15.2±6.6
Night	1.4±0.5	3.2±0.5	19.3±3.0	8.5±1.3
5-Ba Lat				
Day	3.1±1.5	6.5±3.8	18.9±14.6	18.4±10.7
Night	1.3±0.8	3.1±0.8	13.1±2.8	9.9±1.9



Table 4. Relationship between CO₂ outgassing flux with other water quality variables at Hanoi station

Variables	Temp.	DOC	POC	DIC	pCO ₂	pH	Chl-a	%DO	CO ₂ Flux
Temp.	1								
DOC	0.72	1							
POC	0.74	0.53	1						
DIC	-0.99	-0.73	-0.73	1					
pCO₂	-0.11	-0.05	0.00	0.19	1				
pH	-0.90	-0.69	-0.70	0.87	-0.31	1			
Chl_a	0.65	0.29	0.47	-0.65	-0.51	-0.37	1		
%DO	-0.96	-0.70	-0.72	0.97	0.19	0.84	-0.65	1	
CO₂ Flux	0.06	0.17	0.04	-0.02	0.60	-0.31	-0.11	-0.05	1

**Table 5.** CO₂ flux out-gassing in some World Rivers.

River or Tributary	Location	Country	Mean $p\text{CO}_2$ μatm	F_{CO_2} $\text{mmol m}^{-2} \text{day}^{-1}$	$k_{600} \pm \text{SD}$ cm h^{-1}	U_{10} m s^{-1}	References
Red		Vietnam	1,589	28.6 ± 19.3	3.25 ± 0.92	1.2 ± 0.7	This study
Mekong	Downstream	Laos and Cambodia	703 – 1597	88.1 -378.4	12.4 - 44.5	1.3 – 4.9	Alin <i>et al.</i> , 2011
Tonle Sap	Stung Siem Reap	Cambodia	3,066	139.1	5.6 ± 0.9	0.8	Alin <i>et al.</i> , 2011
Tonle Sap	Pousat River	Cambodia	1,404	98.5	10.8 ± 2.8	nd	Alin <i>et al.</i> , 2011
Musi		Indonesia	4,316±928	5 ± 1.1	21.8 ± 4.7	nd	Wit <i>et al.</i> , 2015
Batanghari		Indonesia	2,400±18	1.8 ± 0.4	21.8 ± 4.7	nd	Wit <i>et al.</i> , 2015
Indragiri		Indonesia	5,777±527	9.7 ± 2.2	21.8 ± 4.7	nd	Wit <i>et al.</i> , 2015
Siak		Indonesia	8,555±528	8.3 ± 1.9	22.0 ± 4.7	nd	Wit <i>et al.</i> , 2015
Lupar		Malaysia	1,274±148	13 ± 3.0	26.5 ± 9.3	nd	Wit <i>et al.</i> , 2015
Saribas		Malaysia	1,159±29	14.6 ± 3.3	17.0 ± 13.6	nd	Wit <i>et al.</i> , 2015
Changjiang		China	1,297±901	143	8 - 15	5	Wang <i>et al.</i> , 2007
Maotiao		China	3740	108	10	nd	Wang <i>et al.</i> 2011
Longchuan		China	2,100	156	8	nd	Li <i>et al.</i> , 2012
Yellow		China	$2,810 \pm 1,985$	856 ± 409	42.1 ± 16.9	nd	Ran <i>et al.</i> , 2015
Xijiang		China	2,600	357	15	2.7	Yao <i>et al.</i> , 2007
Negro	South America		$4,260 \pm 1387$	855 ± 294	38.3 ± 19.1	nd	Rasera <i>et al.</i> , 2013
Solimoes			$6,691 \pm 55$	518 ± 17	8.0 ± 2.2		
Arguaia			$2,674 \pm 802$	207 ± 104	9.0 ± 1.8		
Javaes			$3,065 \pm 1208$	156 ± 69	5.0 ± 0.9		
Caxiuana			$4,849 \pm 208$	778 ± 17	20.5 ± 2.5		
Teles Pires			$1,624 \pm 425$	78 ± 43	9.2 ± 2.3		
Cristalino			$3,507 \pm 482$	nd	8.1 ± 1.9		
Krishna			17,205±3500				
Godavari			49,819±1042				
Mahanadi	India		95,859±2234		nd	nd	Sarma <i>et al.</i> , 2012
Ganges			5,029±100				



Gaderu Creek		India	2,215 ± 864 ^a	56.0 ± 100.9	4 ± 5	1.4 ± 1.9	<i>Borges et al., 2003</i>
Rhone		France	2,015±944	nd	15	nd	<i>Cole et al., 2001</i>
Negro	South America		4,260±1387	855±294	38.3±19.1		<i>Rasera et al., 2013</i>
Solimoes			6,691±55	518±17	8.0±2.2		
Arguaia			2,674±802	207±104	9.0±1.8		
Javaes			3,065±1208	156±69	5.0±0.9	nd	
Caxiuana			4,849±208	778±17	20.5±2.5		
Teles Pires			1,624±425	78±43	9.2±2.3		
Cristalino			3,507±482	nd	8.1±1.9		
Capibaribe	Coastal region of the State of Pernambuco	Brazil	8,340	225	nd	2.2	<i>Moacyr et al., 2013</i>
Hudson		USA	1,125±403	nd	4.1	3.5± 2.0	<i>Raymond et al., 1997</i>
	Upper	North America	1,220 ± 9.1	6	1.25	nd	
Yukon	Middle		1,890 ± 9.9	62	7.92	nd	<i>Striegl et al., 2007; 2012</i>
	Lower		3,090 ± 16.5	193	15	nd	
Ottawa		Canada	1,200	80.8	4	nd	<i>Telmer and Veizer, 1999</i>
Amazon			4,350 ± 1900	190 ± 55	9.6 ± 3.8	1 - 3	<i>Richey et al., 2002</i>
Mississippi			100 - 600	270	3.9	5.3	<i>Dubois et al., 2010; Lohrenz and Cai, 2006</i>
Nagada Creek	The northern Papua New Guinea coast		799 ± 357 ^a	43.6 ± 33.2	8 ± 6	3.0 ± 2.1	<i>Borges et al., 2003</i>
Norman's Pond	Bahamas archipelago		165 ± 86 ^a	13.8 ± 8.3	13 ± 3	5.5 ± 1.3	<i>Borges et al., 2003</i>

^a calculated the values for the $p\text{CO}_2$ Water-Air Gradient ($\Delta p\text{CO}_2$ in μatm)

nd. No data



List of figures

Figure 1: The Red River system and sampling sites.

Figure 2: Spatial and seasonal variation of different environmental variables in the Red River system in 2014

Figure 3: Comparison the result of riverine $p\text{CO}_2$ of the lower Red River by measured (equilibrator) and calculated ($\text{CO}_2\text{-SYS}$) methods

Figure 4: Spatial and seasonal variation of CO_2 flux out-gassing in the Red River system in 2014.

Figure 5: Relationship between $p\text{CO}_2$, $f\text{CO}_2$ and water temperature at 5 sites observed of the lower Red River in dry season in 2014

Figure 6: Relationship between environmental variables and $p\text{CO}_2$ or CO_2 flux at five sites of the Red River.

Figure 7: Relationship between $p\text{CO}_2$, $f\text{CO}_2$ and river discharge at 5 sites observed of the lower Red River in wet and dry season in 2014.

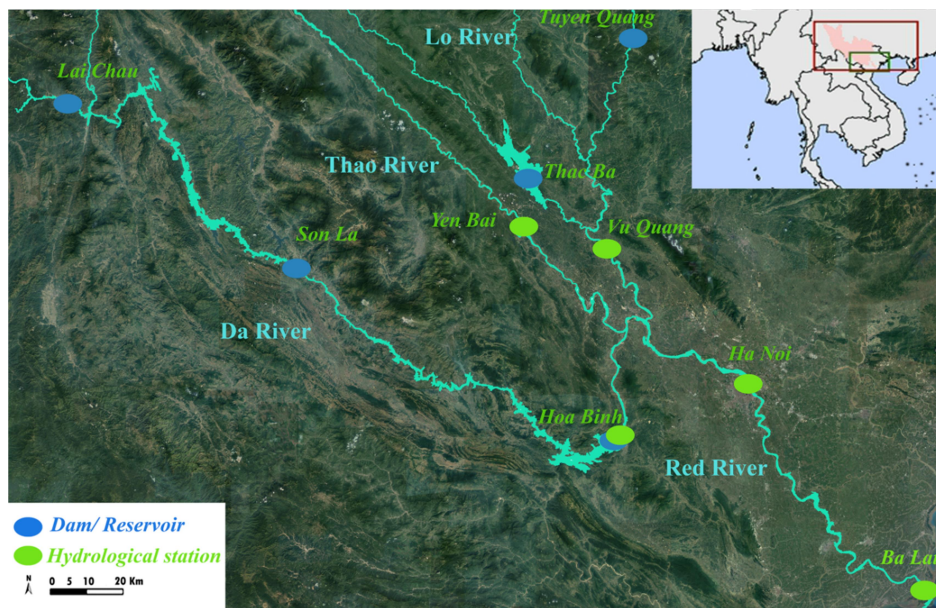


Figure 1. The Red River system and sampling sites

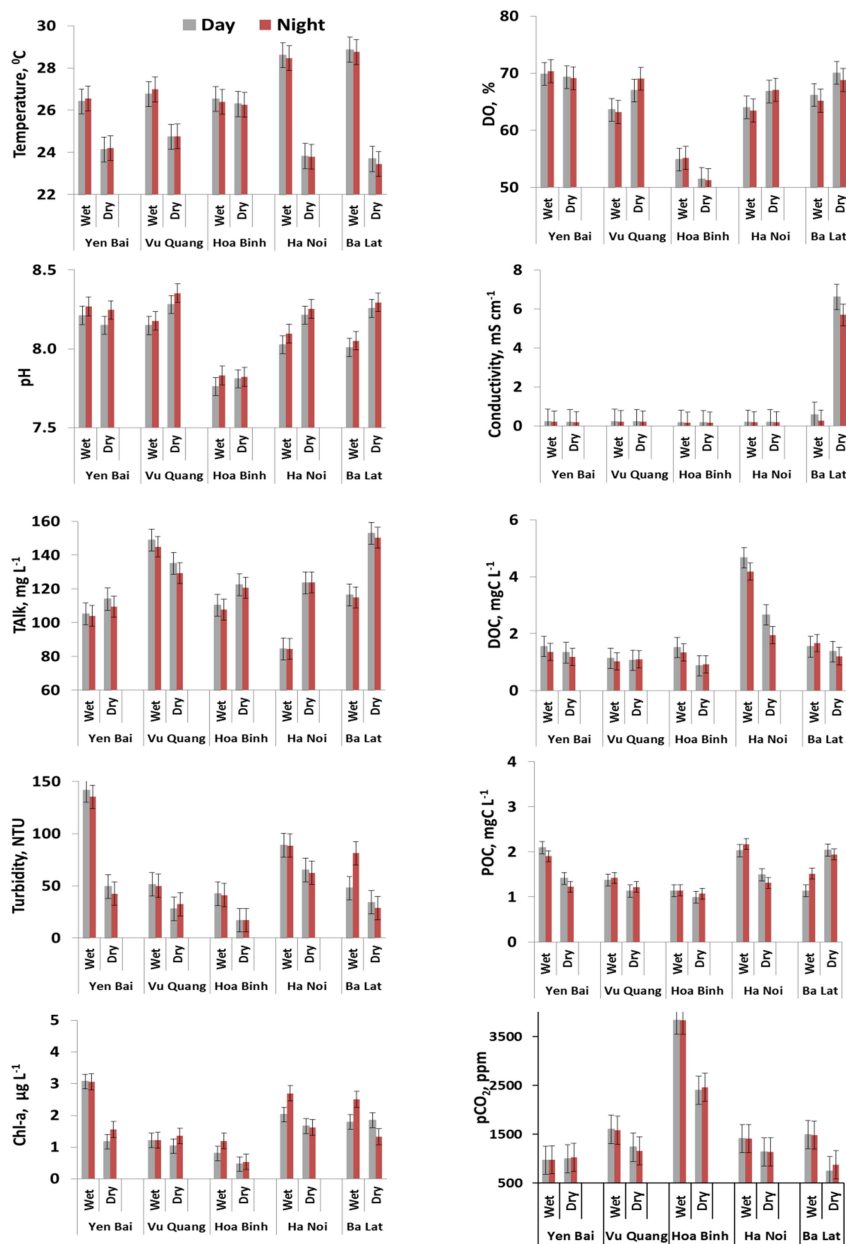
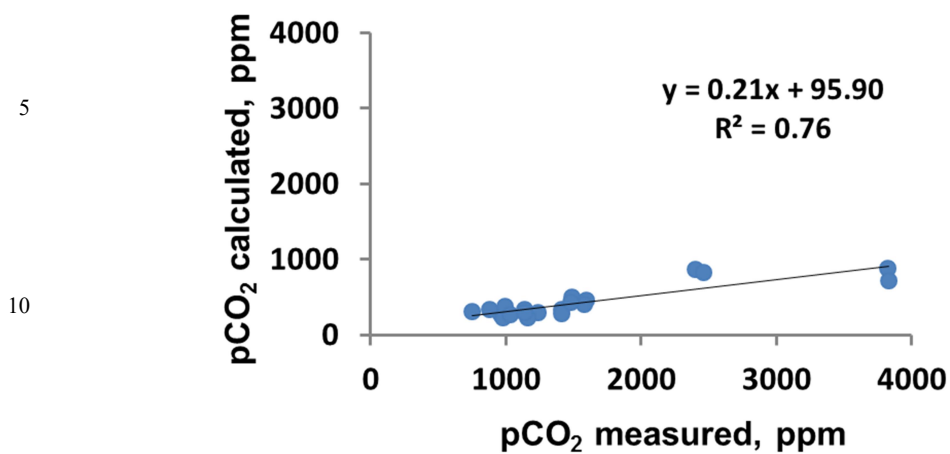
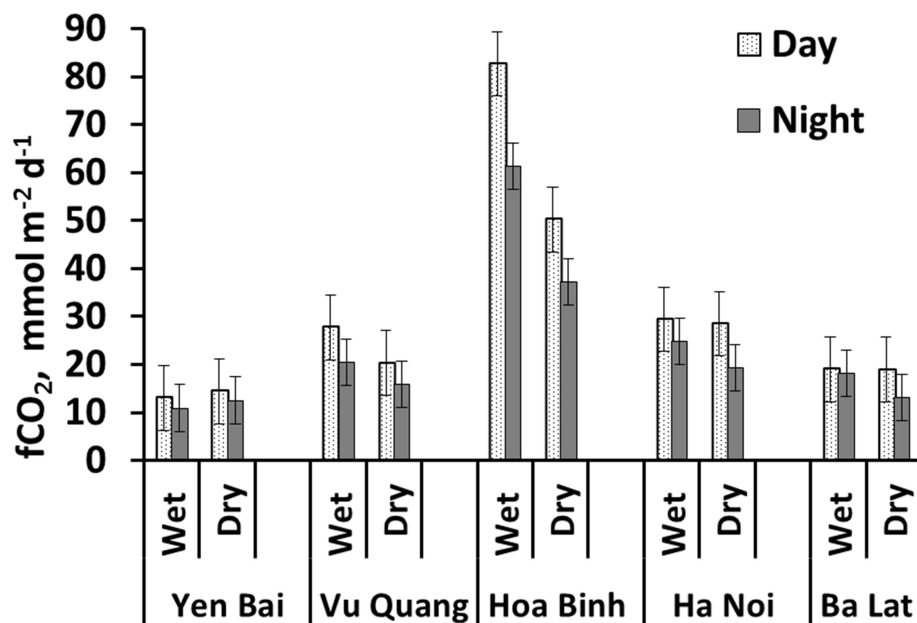


Figure 2. Spatial and seasonal variation of different environmental variables in the Red River system in 2014



15 Figure 3. Comparison the result of riverine pCO₂ of the lower Red River by measured (equilibrator) and calculated (CO₂_SYS) methods



5

Figure 4. Spatial and seasonal variation of CO₂ flux out-gassing in the Red River system in 2014.

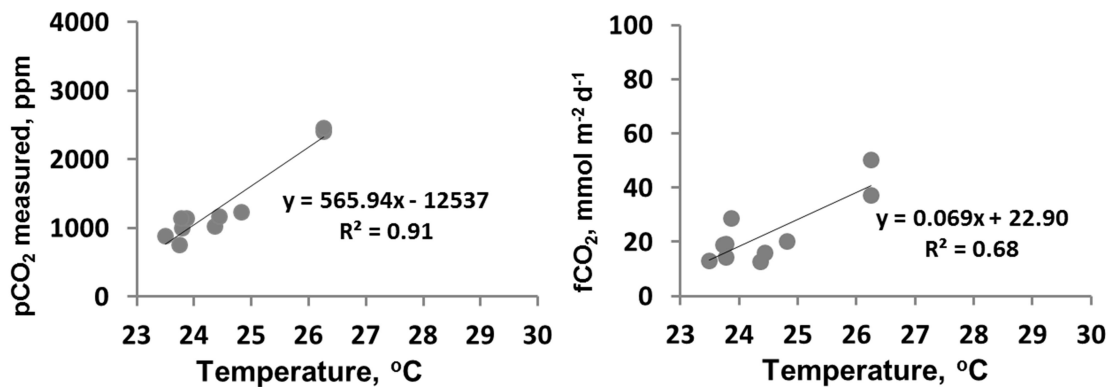


Figure 5. Relationship between $p\text{CO}_2$, $f\text{CO}_2$ and water temperature at 5 sites observed of the lower Red River in dry season in 2014.

5

10

15

20



5

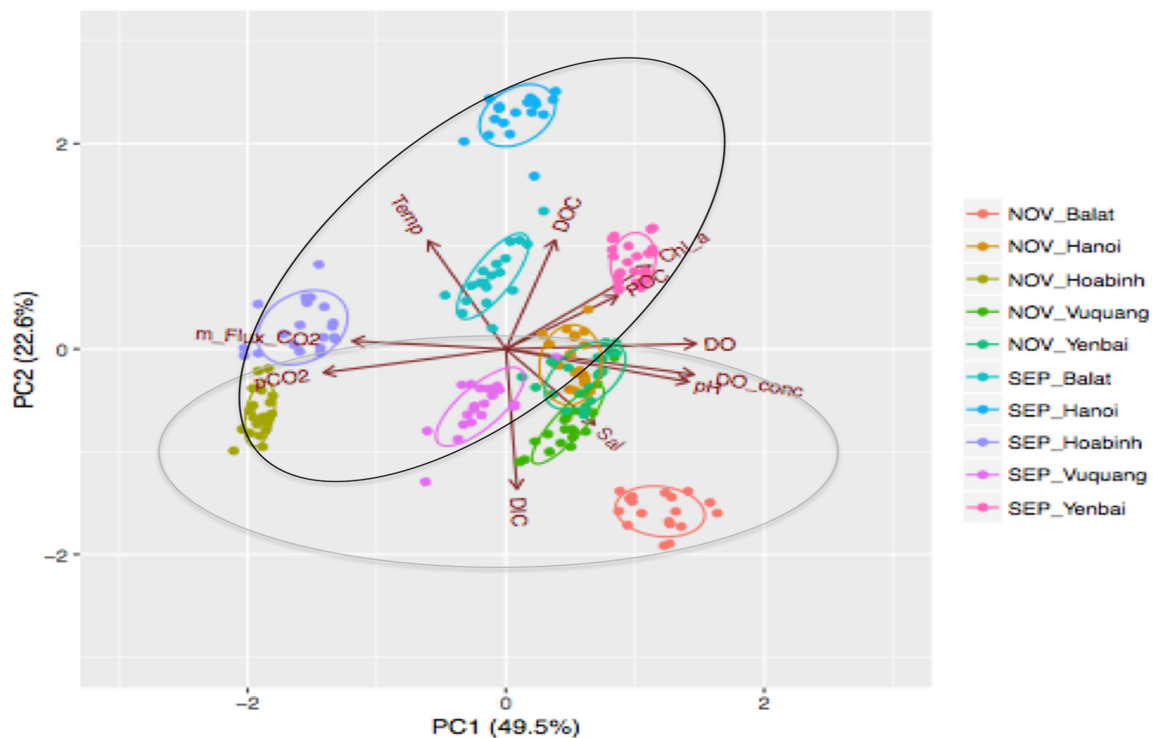


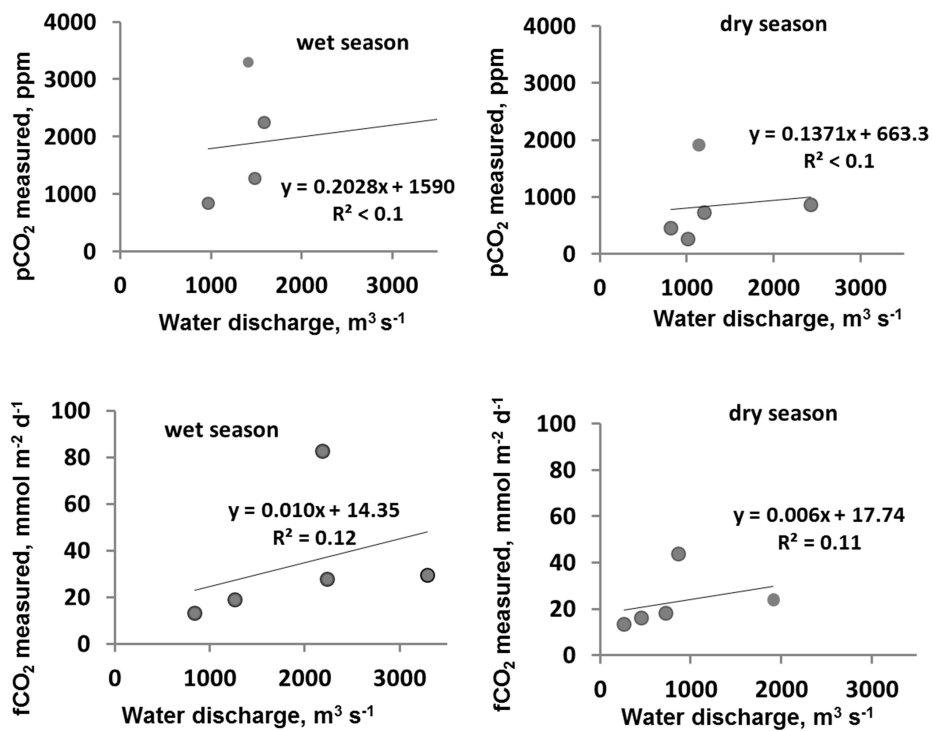
Figure 6. Relationship between environmental variables and $p\text{CO}_2$ or CO_2 flux at five sites of the Red River

10

15



5



10 Figure 7. Relationship between $p\text{CO}_2$, $f\text{CO}_2$ and river discharge at 5 sites observed of the lower Red River in wet and dry season in 2014.